

Title: Quantum transport in one dimension: from integrability to many-body localization and topology

Date: Apr 23, 2013 11:00 AM

URL: <http://pirsa.org/13040125>

Abstract: Recent advances in analytical theory and numerical methods enable some long-standing questions about transport in one dimension to be answered; these questions are closely related to transport experiments in quasi-1D compounds. The spinless fermion chain with nearest-neighbor interactions at half-filling, or equivalently the XXZ model in zero magnetic field, is an example of an integrable system in which no conventional conserved quantity forces dissipationless transport (Drude weight); we show that there is nevertheless a Drude weight and that at some points its contribution is from a new type of conserved quantity recently constructed by Prosen. Adding an integrability-breaking perturbation leads to a scaling theory of conductivity at low temperature. Adding disorder, we study the question of how Anderson localization is modified by interactions when the system remains fully quantum coherent ("many-body localization"). We find that even weak interactions are a singular perturbation on some quantities: entanglement grows slowly but without limit, suggesting that dynamics in the possible many-body localized phase are glass-like. If time permits, some results on the fractional Luttinger's theorem and the 1D limit of quantum Hall states will be presented.

Outline



1. Introduction

Some key ideas of the DMRG “renaissance”, 2005-present

Entanglement spectra to characterize criticality & convergence

2. Integrability in 1D systems and its consequences for transport

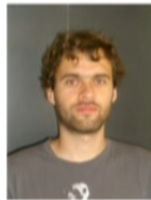
(C. Karrasch, J. Bardarson, JEM, PRL 2012)

Conductivity scaling in almost integrable chains

(Yichen Huang, C. Karrasch, JEM, in preparation)

3. Entanglement growth in models of many-body localization

(J. Bardarson, F. Pollmann, JEM, PRL 2012).



Jens Bardarson



Christoph Karrasch



Frank Pollmann

Studying quantum correlations with classical algorithms: applied entanglement entropy

Basic (hazy) concept: "Entanglement entropy determines how much classical information is required to describe a quantum state."

Example:

how many classical real numbers are required to describe a *product* (not entangled) state of N spins?

simple product $|\psi\rangle = A_{s_1} A_{s_2} A_{s_3} A_{s_4} |s_1 s_2 s_3 s_4\rangle$

Answer: $\sim N$ (versus exponentially many for a general state)

How do we efficiently manipulate/represent moderately entangled states?

Applied entanglement entropy

The remarkable success of the density-matrix renormalization group algorithm in one dimension (White, 1992; Ostlund and Rommer, 1995) can be understood as follows:

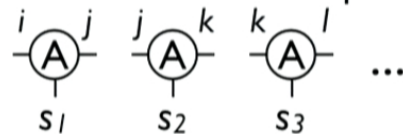
DMRG constructs “matrix product states” that retain local entanglement but throw away long-ranged entanglement.

Example states for four spins:

simple product $|\psi\rangle = A_{s_1} A_{s_2} A_{s_3} A_{s_4} |s_1 s_2 s_3 s_4\rangle$

matrix product $|\psi\rangle = A_{s_1}^{ij} A_{s_2}^{jk} A_{s_3}^{kl} A_{s_4}^{li} |s_1 s_2 s_3 s_4\rangle$

Graphical tensor network representation:



Applied entanglement entropy

The remarkable success of the density-matrix renormalization group algorithm in one dimension (White, 1992; Ostlund and Rommer, 1995) can be understood as follows:

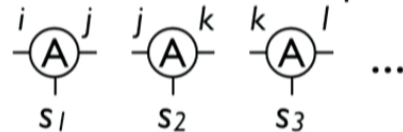
DMRG constructs “matrix product states” that retain local entanglement but throw away long-ranged entanglement.

Example states for four spins:

simple product $|\psi\rangle = A_{s_1} A_{s_2} A_{s_3} A_{s_4} |s_1 s_2 s_3 s_4\rangle$

matrix product $|\psi\rangle = A_{s_1}^{ij} A_{s_2}^{jk} A_{s_3}^{kl} A_{s_4}^{li} |s_1 s_2 s_3 s_4\rangle$

Graphical tensor network representation:



“Infinite system” methods

Note that we can impose translation invariance simply by requiring constant matrices A .

In other words, for quantities in a translation-invariant system, we *just calculate A , rather than a large finite system.*

(Idea 1 of renaissance; see Vidal '07, for example)

matrix product $|\psi\rangle = A_{s_1}^{ij} A_{s_2}^{jk} A_{s_3}^{kl} A_{s_4}^{li} |s_1 s_2 s_3 s_4\rangle$

So where is the approximation?

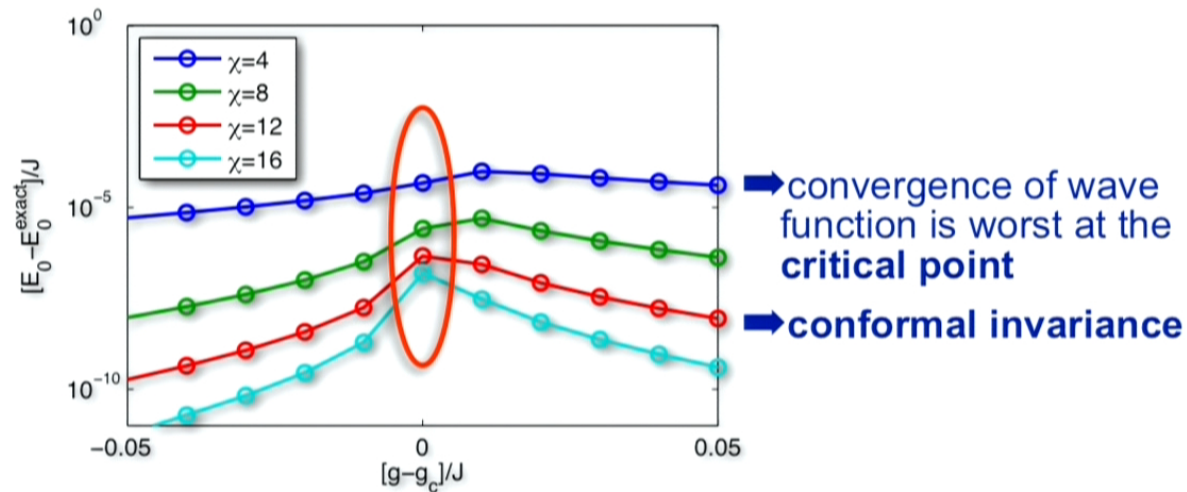
A finite matrix A can only capture a finite amount of entanglement.

In the early DMRG days, it was often thought:

1. To study an infinite system, we should study a large finite one.
2. Gapless/critical systems are hard
3. Dynamical properties are hard
4. Finite temperature is hard

But none of these is strictly correct.

- find the ground state of a system by using **imaginary time evolution** (almost unitary for small time steps)
- parallel updates for **infinite/translational invariant** systems: **iTEBD** [Vidal '07]
- **example**, transverse Ising model: $H = \sum_i (J\sigma_i^z\sigma_{i+1}^z + g\sigma_i^x)$



Criticality: finite-entanglement scaling

All numerical methods have difficulty with quantum critical points. In DMRG-type approaches, this can be understood from the divergence of entanglement entropy at such points: the entanglement in a matrix product state is limited by $\dim A$.

matrix product $|\psi\rangle = A_{s_1}^{ij} A_{s_2}^{jk} A_{s_3}^{kl} A_{s_4}^{li} |s_1 s_2 s_3 s_4\rangle$

Quantitatively, it is found that $\dim A$ plays a role similar to imposing a finite system size:

(Tagliacozzo et al., PRB 2008). $L_{\text{eff}} \propto \chi^\kappa, \quad \chi = \dim A$

Finite matrix dimension effectively moves the system away from the critical point.

What determines this “finite-entanglement scaling”?

Is it like “finite-size scaling” of CFT’s (cf. Blöte, Cardy, & Nightingale)

A way to picture the entanglement of a state

- **Schmidt decomposition** of the state (**SVD**):

$$\begin{aligned} |\psi\rangle &= \sum_{i=1}^{N_A} \sum_{j=1}^{N_B} C_{ij} |i\rangle_A |j\rangle_B \\ &= \sum_{\alpha=1}^{\min(N_A, N_B)} \lambda_{\alpha} |\phi_{\alpha}\rangle_A |\phi_{\alpha}\rangle_B \end{aligned}$$



with $\lambda_{\alpha} \geq 0$ and $\sum_{\alpha} \lambda_{\alpha}^2 = 1$

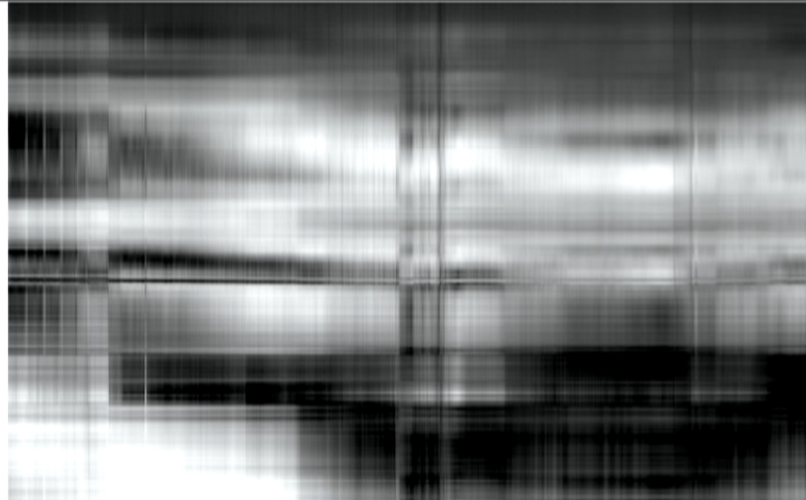
- a natural measure of the entanglement is the **entropy**:

$$S_A = S_B = S = - \sum_{\alpha} \lambda_{\alpha}^2 \log(\lambda_{\alpha}^2)$$

Efficient representation of quantum states?

- Hilbert-space dimension of many-body problems increases **exponentially** with number of sites
example: spin 1/2 system on “classical” computers
(store **one state** in double precision)
- need an efficient way to “**compress**” quantum states so that the matrices studied remain finite-dimensional
 - ➔ slightly entangled 1D systems: **Matrix Product States**
 - ➔ DMRG, TEBD, ...

$\chi = 4$



$\chi = 16$



$\chi = 64$



$\chi = 256$



- (Li-Haldane) “entanglement spectrum” [Calabrese et al ‘08]

$$n(\lambda) = I_0 \left(2\sqrt{-b^2 - 2b \log \lambda} \right) \quad \# \text{ of } \hat{\lambda} \text{'s greater than } \lambda$$

$$\text{with } b = \frac{S}{2} = \frac{c}{12} \log \xi = -2 \log \lambda_{\max}$$

continuum of Schmidt values $|\psi\rangle = \sum_{\alpha=1}^{\infty} \lambda_{\alpha} |\phi_{\alpha}\rangle_A |\phi_{\alpha}\rangle_B$

- Want to explain how at a critical point, finite matrix size χ effectively moves the system away from criticality, leading to universal relations like

$$L_{\text{eff}} \propto \chi^{\kappa}, \quad \chi = \dim A$$

- **A heuristic argument** for the asymptotic case
(using a continuum of Schmidt values and $\chi \rightarrow \infty$)

➡ **universal finite-entanglement scaling relations**

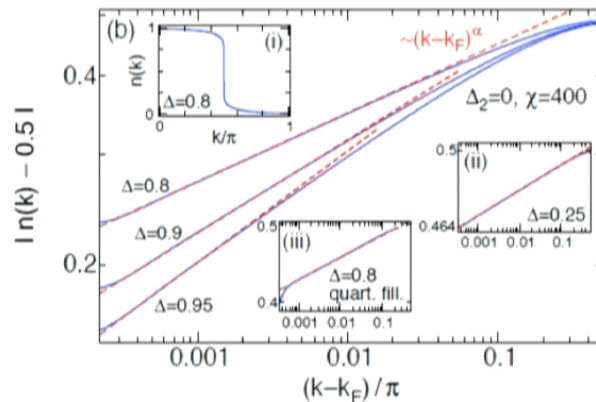
$$\kappa = \frac{6}{c \left(\sqrt{\frac{12}{c} + 1} \right)} \Rightarrow S = \frac{1}{\sqrt{\frac{12}{c} + 1}} \log \chi$$

F. Pollmann, S. Mukerjee, A. Turner, and J.E. Moore, PRL 2009
Some checks for various critical theories are in that paper, and the recent work
B. Pirvu, G. Vidal, F. Verstraete, L. Tagliacozzo, arXiv:1204.3934

So critical points are worse than gapped points, but in a controlled way.
What does this mean in practice?

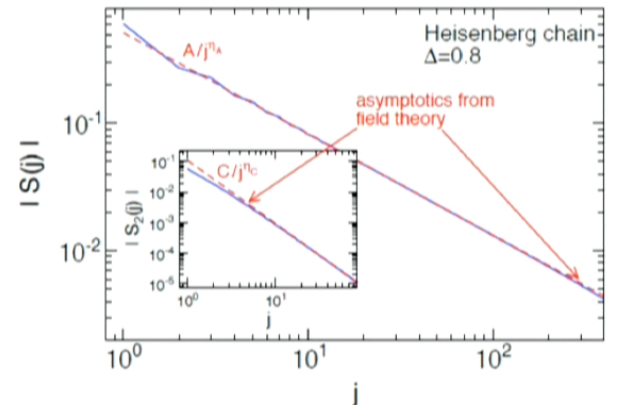
Remark: Entanglement spectra are qualitatively different for random critical spin chains
than for pure ones, though entanglement entropies similar (M. Fagotti, P. Calabrese, JEM).

Tests of Luttinger liquid behavior in the XXZ model



Momentum distribution $n(k)$

(C. Karrasch and JEM, PRB)



Check of leading staggered and uniform correlators against Lukyanov and Terras

Next: try to solve an open problem of dynamical properties at finite temperature.
At end: return to statics in chiral Luttinger liquids

Dissipationless transport

When is there a nonzero Drude weight D ?

$$\sigma(\omega) = D\delta(\omega) + \dots$$

Two easy examples:

I. Superconductors (transport by condensate)

II. Part of the current is conserved: Mazur lower bound

$$D = \frac{1}{2LT} \lim_{t \rightarrow \infty} \langle J(t)J(0) \rangle \geq \frac{1}{2LT} \sum_k \frac{\langle JQ_k \rangle^2}{\langle Q_k^2 \rangle}$$

Dissipationless transport

When is there a nonzero Drude weight D ?

$$\sigma(\omega) = D\delta(\omega) + \dots$$

Two easy examples:

I. Superconductors (transport by condensate)

II. Part of the current is conserved: Mazur lower bound

$$D = \frac{1}{2LT} \lim_{t \rightarrow \infty} \langle J(t)J(0) \rangle \geq \frac{1}{2LT} \sum_k \frac{\langle JQ_k \rangle^2}{\langle Q_k^2 \rangle}$$

Dissipationless transport

When is there a nonzero Drude weight D ?

$$\sigma(\omega) = D\delta(\omega) + \dots$$

Example of Mazur bound: suppose momentum is conserved, and current is proportional to momentum (e.g., if only one kind of particle).

Technical note: the Drude weight is not thermodynamic:

$$D = \frac{1}{L} \left[\langle \Theta \rangle - \hbar \sum_{n,m} (1 - \delta_{\epsilon_n, \epsilon_m}) \frac{e^{-\beta\epsilon_n} - e^{-\beta\epsilon_m}}{Z(\epsilon_m - \epsilon_n)} |\langle n|J|m \rangle|^2 \right], \quad D_m = \frac{1}{L} \left[\langle \Theta \rangle - \hbar \sum_{n,m} \frac{e^{-\beta\epsilon_n} - e^{-\beta\epsilon_m}}{Z(\epsilon_m - \epsilon_n)} |\langle n|J|m \rangle|^2 \right]$$

where D_m is “Meissner stiffness” (response to flux). Always $D \geq D_m$. (Mukerjee and Shastry, PRB 2007). Here

$$\Theta = \lim_{k \rightarrow 0} \frac{1}{k} [\rho(k), J(-k)]$$

$$\sigma(\omega) = D\delta(\omega) + \dots$$

$$D = \frac{1}{2LT} \lim_{t \rightarrow \infty} \langle J(t)J(0) \rangle \geq \frac{1}{2LT} \sum_k \frac{\langle JQ_k \rangle^2}{\langle Q_k^2 \rangle}$$

What about “integrable” models with an infinite number of conserved local quantities, none of which gives a lower bound?

Actually this happens quite often in 1D--simplest case is spinless interacting fermions (XXZ model in zero magnetic field).

$$H = \sum_i [J_{xx}(S_i^x S_{i+1}^x + S_i^y S_{i+1}^y) + \Delta S_i^z S_{i+1}^z + hS_i^z]$$

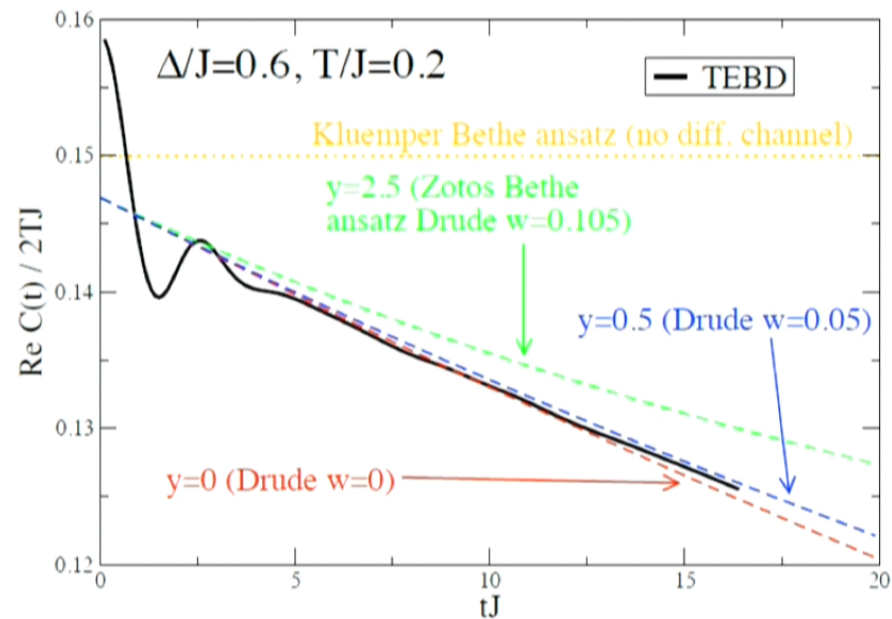
The Drude weight is easy to calculate and nonzero at $T=0$.
20+ years of efforts to calculate it (or even prove that it is nonzero) at $T>0$, $h=0$, by either analytical or numerical methods.

(cf. Sirker, Pereira, Affleck, PRB 2011)

$$\sigma(\omega) = D\delta(\omega) + \dots$$

$$D = \frac{1}{2LT} \lim_{t \rightarrow \infty} \langle J(t)J(0) \rangle \geq \frac{1}{2LT} \sum_k \frac{\langle JQ_k \rangle^2}{\langle Q_k^2 \rangle}$$

data from Sirker, Pereira, Affleck, PRB 2011



$$\sigma(\omega) = D\delta(\omega) + \dots$$

$$D = \frac{1}{2LT} \lim_{t \rightarrow \infty} \langle J(t)J(0) \rangle \geq \frac{1}{2LT} \sum_k \frac{\langle JQ_k \rangle^2}{\langle Q_k^2 \rangle}$$

What about “integrable” models with an infinite number of conserved local quantities, none of which gives a lower bound?

Actually this happens quite often in 1D--simplest case is spinless interacting fermions (XXZ model in zero magnetic field).

$$H = \sum_i [J_{xx}(S_i^x S_{i+1}^x + S_i^y S_{i+1}^y) + \Delta S_i^z S_{i+1}^z + hS_i^z]$$

The Drude weight is easy to calculate and nonzero at $T=0$.
20+ years of efforts to calculate it (or even prove that it is nonzero) at $T>0$, $h=0$, by either analytical or numerical methods.

(cf. Sirker, Pereira, Affleck, PRB 2011)

$$\sigma(\omega) = D\delta(\omega) + \dots$$

$$D = \frac{1}{2LT} \lim_{t \rightarrow \infty} \langle J(t)J(0) \rangle \geq \frac{1}{2LT} \sum_k \frac{\langle JQ_k \rangle^2}{\langle Q_k^2 \rangle}$$

What about “integrable” models with an infinite number of conserved local quantities, none of which gives a lower bound?

Actually this happens quite often in 1D--simplest case is spinless interacting fermions (XXZ model in zero magnetic field).

$$H = \sum_i [J_{xx}(S_i^x S_{i+1}^x + S_i^y S_{i+1}^y) + \Delta S_i^z S_{i+1}^z + hS_i^z]$$

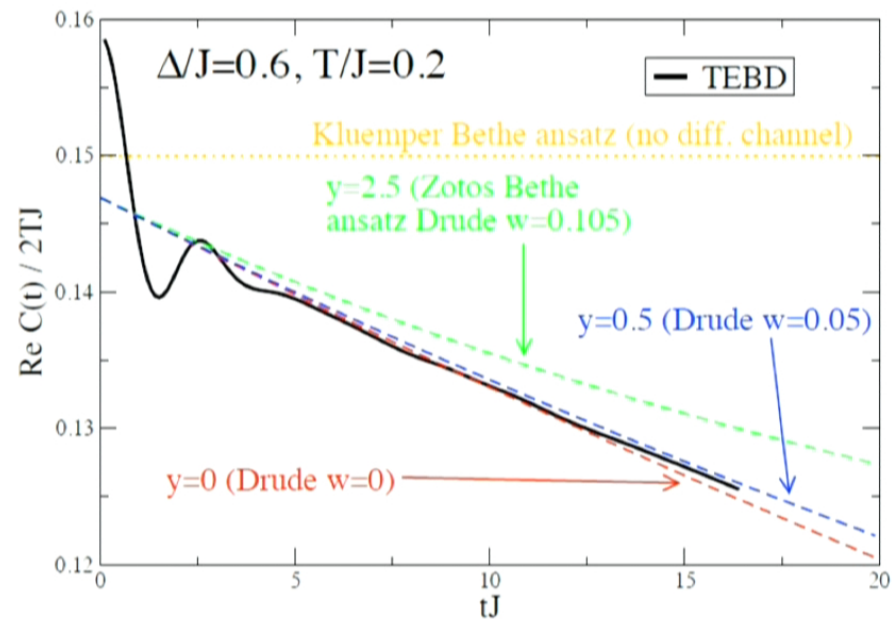
The Drude weight is easy to calculate and nonzero at $T=0$.
20+ years of efforts to calculate it (or even prove that it is nonzero) at $T>0$, $h=0$, by either analytical or numerical methods.

(cf. Sirker, Pereira, Affleck, PRB 2011)

$$\sigma(\omega) = D\delta(\omega) + \dots$$

$$D = \frac{1}{2LT} \lim_{t \rightarrow \infty} \langle J(t)J(0) \rangle \geq \frac{1}{2LT} \sum_k \frac{\langle JQ_k \rangle^2}{\langle Q_k^2 \rangle}$$

data from Sirker, Pereira, Affleck, PRB 2011



Dissipationless transport

When is there a nonzero Drude weight D ?

$$\sigma(\omega) = D\delta(\omega) + \dots$$

Example of Mazur bound: suppose momentum is conserved, and current is proportional to momentum (e.g., if only one kind of particle).

Technical note: the Drude weight is not thermodynamic:

$$D = \frac{1}{L} \left[\langle \Theta \rangle - \hbar \sum_{n,m} (1 - \delta_{\epsilon_n, \epsilon_m}) \frac{e^{-\beta\epsilon_n} - e^{-\beta\epsilon_m}}{Z(\epsilon_m - \epsilon_n)} |\langle n|J|m \rangle|^2 \right], \quad D_m = \frac{1}{L} \left[\langle \Theta \rangle - \hbar \sum_{n,m} \frac{e^{-\beta\epsilon_n} - e^{-\beta\epsilon_m}}{Z(\epsilon_m - \epsilon_n)} |\langle n|J|m \rangle|^2 \right]$$

where D_m is “Meissner stiffness” (response to flux). Always $D \geq D_m$. (Mukerjee and Shastry, PRB 2007). Here

$$\Theta = \lim_{k \rightarrow 0} \frac{1}{k} [\rho(k), J(-k)]$$

Some progress, 2011-present

$$\sigma(\omega) = D\delta(\omega) + \dots$$
$$D = \frac{1}{2LT} \lim_{t \rightarrow \infty} \langle J(t)J(0) \rangle \geq \frac{1}{2LT} \sum_k \frac{\langle JQ_k \rangle^2}{\langle Q_k^2 \rangle}$$

Prosen: there is an iterative process to construct a nonlocal quantity that gives a lower bound that depends non-analytically on anisotropy, with cusps at $\Delta = \cos(\pi/n)$. (PRL 2011)

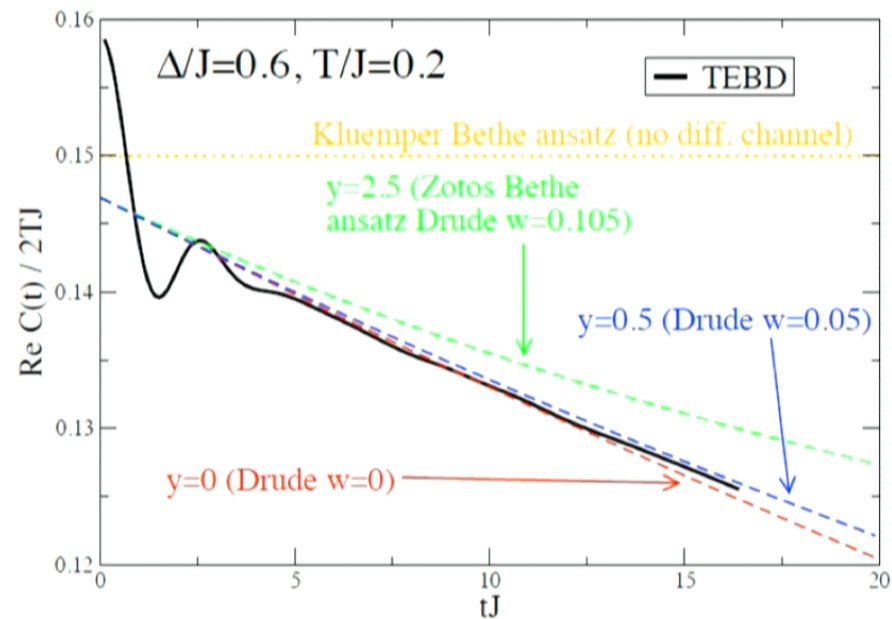
Karrasch-Bardarson-JEM: The Drude weight can be calculated numerically for all but the lowest temperatures at positive Δ , and essentially all temperatures at negative Δ .

The lower bound appears to saturate the full value at the cusps.

$$\sigma(\omega) = D\delta(\omega) + \dots$$

$$D = \frac{1}{2LT} \lim_{t \rightarrow \infty} \langle J(t)J(0) \rangle \geq \frac{1}{2LT} \sum_k \frac{\langle JQ_k \rangle^2}{\langle Q_k^2 \rangle}$$

data from Sirker, Pereira, Affleck, PRB 2011



Some progress, 2011-present

$$\sigma(\omega) = D\delta(\omega) + \dots$$
$$D = \frac{1}{2LT} \lim_{t \rightarrow \infty} \langle J(t)J(0) \rangle \geq \frac{1}{2LT} \sum_k \frac{\langle JQ_k \rangle^2}{\langle Q_k^2 \rangle}$$

Prosen: there is an iterative process to construct a nonlocal quantity that gives a lower bound that depends non-analytically on anisotropy, with cusps at $\Delta = \cos(\pi/n)$. (PRL 2011)

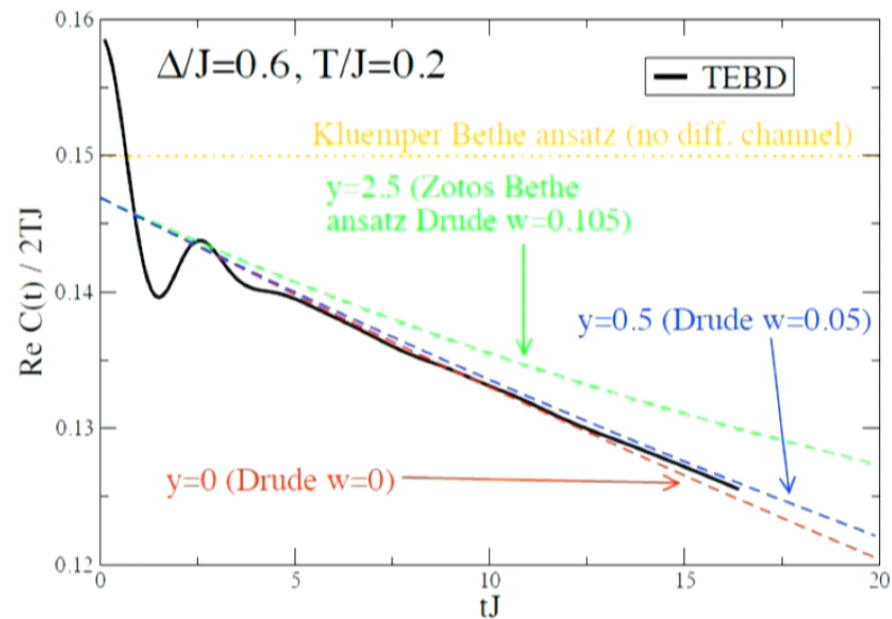
Karrasch-Bardarson-JEM: The Drude weight can be calculated numerically for all but the lowest temperatures at positive Δ , and essentially all temperatures at negative Δ .

The lower bound appears to saturate the full value at the cusps.

$$\sigma(\omega) = D\delta(\omega) + \dots$$

$$D = \frac{1}{2LT} \lim_{t \rightarrow \infty} \langle J(t)J(0) \rangle \geq \frac{1}{2LT} \sum_k \frac{\langle JQ_k \rangle^2}{\langle Q_k^2 \rangle}$$

data from Sirker, Pereira, Affleck, PRB 2011



Some progress, 2011-present

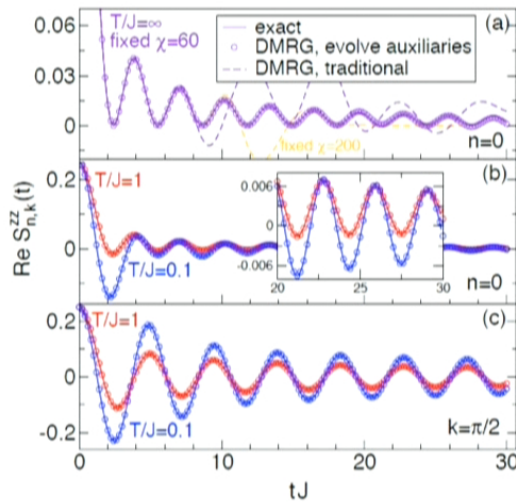
$$\sigma(\omega) = D\delta(\omega) + \dots$$
$$D = \frac{1}{2LT} \lim_{t \rightarrow \infty} \langle J(t)J(0) \rangle \geq \frac{1}{2LT} \sum_k \frac{\langle JQ_k \rangle^2}{\langle Q_k^2 \rangle}$$

Prosen: there is an iterative process to construct a nonlocal quantity that gives a lower bound that depends non-analytically on anisotropy, with cusps at $\Delta = \cos(\pi/n)$. (PRL 2011)

Karrasch-Bardarson-JEM: The Drude weight can be calculated numerically for all but the lowest temperatures at positive Δ , and essentially all temperatures at negative Δ .

The lower bound appears to saturate the full value at the cusps.

Finite-temperature dynamics check

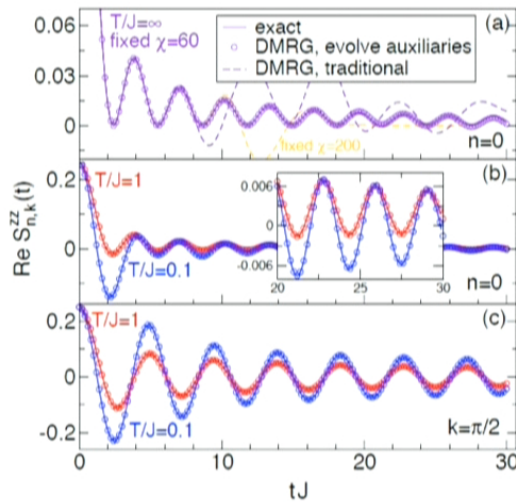


Trick: (Karrasch-Bardarson)

Finite-temperature dynamics are simulated by pure state evolution of a system with $2N$ spins. There is an arbitrariness in the unitary evolution of the “ancilla” spins.

The entanglement growth can be minimized if the ancilla spins evolve under the time-reversal conjugate of the unitary evolution of the physical spins.

Finite-temperature dynamics check



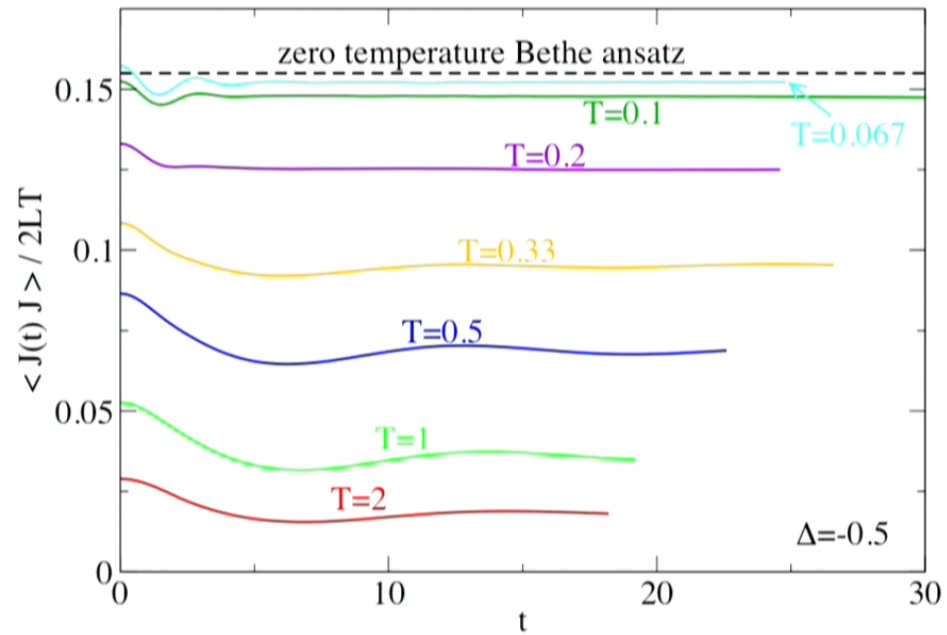
Trick: (Karrasch-Bardarson)

Finite-temperature dynamics are simulated by pure state evolution of a system with $2N$ spins. There is an arbitrariness in the unitary evolution of the “ancilla” spins.

The entanglement growth can be minimized if the ancilla spins evolve under the time-reversal conjugate of the unitary evolution of the physical spins.

Drude weight of XXZ model

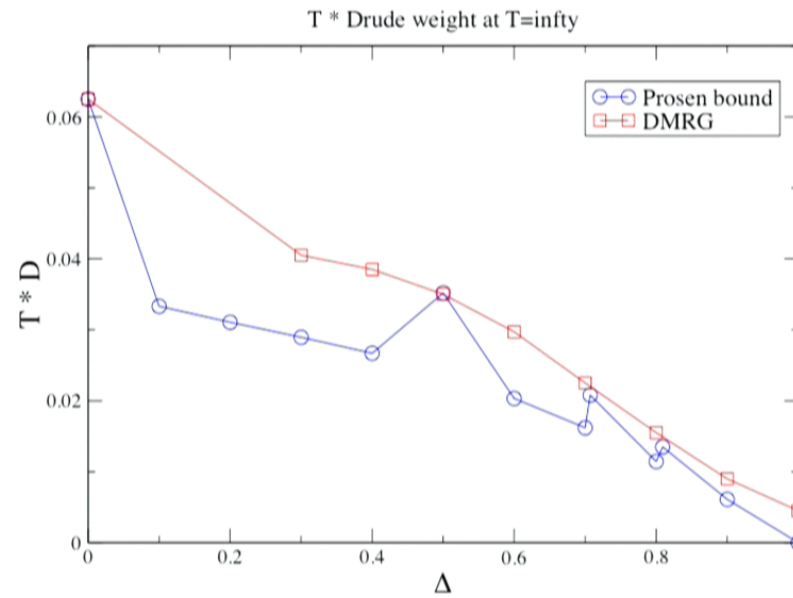
$$\sigma(\omega) = D\delta(\omega) + \dots$$



Time-dependent matrix-product-state numerics using an "entanglement-based" trick

Why?

Connection to lower bound from “nonlocal” conserved quantity at high T:
saturation at cusps $\Delta = \cos(\pi/n)$



(Karrasch, Bardarson, JEM, PRL 2012; thanks J. Sirker)

Lesson

Without disorder, transport can be very sensitive to integrability--*gapless* integrable models seem to have nonzero Drude weight in general.

The “nonlocal” conserved quantities are actually important for basic questions. Currently computing *conductivity* in massless non-integrable and massive cases.

1. add staggered field to break integrability and study scaling of conductivity in *gapless* regime.

(Y. Huang, C. Karrasch, JEM, arXiv)

2. consider non-equilibrium: when is there a steady state? does Fourier’s law apply?

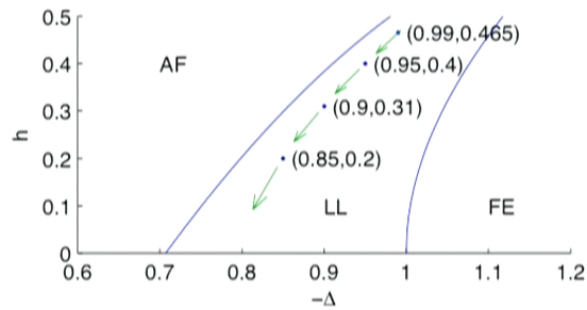
(C. Karrasch, R. Ilan, JEM, arXiv)

3. add random field to break integrability, and study “many-body localization” in XXZ models with random fields

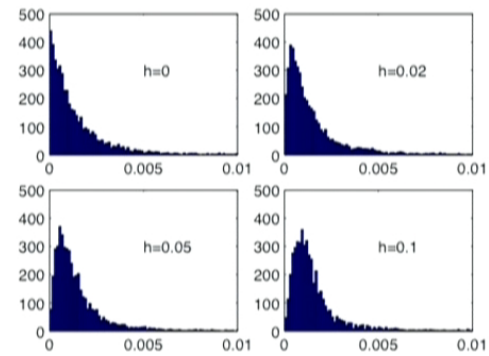
(J. Bardarson, F. Pollmann, JEM, PRL 2012)

Staggered field and non-integrability

$$H = \sum_{i=1}^L \left[S_i^x S_{i+1}^x + S_i^y S_{i+1}^y + \Delta S_i^z S_{i+1}^z + (-1)^i h S_i^z \right]$$



In one region, of the phase diagram, h is irrelevant (system remains Luttinger liquid), and we can track RG flow



Level statistics become Wigner-Dyson (level repulsion) rather than Poisson

Staggered field and non-integrability

$$H = \sum_{i=1}^L \left[S_i^x S_{i+1}^x + S_i^y S_{i+1}^y + \Delta S_i^z S_{i+1}^z + (-1)^i h S_i^z \right]$$

Bosonization analysis: h just generates a new cosine:

$$H = \frac{v}{2} \int dx \left(\Pi^2 + (\partial_x \phi)^2 \right) + ch \int dx \cos \left(2\sqrt{\pi K} \phi \right) + \dots,$$

where ellipses indicate Umklapp and band-curvature terms present in the XXZ model.

We know that simple bosonization analysis of the Umklapp term is actually incorrect, because integrability leads to a non-zero Drude weight.

Does adding the new cosine make the scaling prediction valid?

$$\sigma_c = h^{-2} T^{3-2K} / C(K)$$

$$\begin{aligned} C(K) &= \pi^{K-3} (1 - K^{-1}/2)^{2K-1} \cos^2(\pi K/2) \\ &\quad \times \sin^{1-2K}(\pi K^{-1}/2) \Gamma^2(K/2) \Gamma^2(1/2 - K/2) \\ &\quad \times \Gamma^{2K} \left(\frac{1}{4K-2} \right) \Gamma^{-2K} \left(\frac{1}{2-K^{-1}} \right) \exp \left(2 \int_0^{+\infty} \frac{dx}{x} \right. \\ &\quad \left. \times \left(1 - (K-1)e^{-2x} - \frac{\sinh x}{\sinh((K^{-1}-1)x + \sinh x)} \right) \right). \end{aligned}$$

Staggered field and non-integrability

$$H = \sum_{i=1}^L \left[S_i^x S_{i+1}^x + S_i^y S_{i+1}^y + \Delta S_i^z S_{i+1}^z + (-1)^i h S_i^z \right]$$

Bosonization analysis: h just generates a new cosine:

$$H = \frac{v}{2} \int dx \left(\Pi^2 + (\partial_x \phi)^2 \right) + ch \int dx \cos \left(2\sqrt{\pi K} \phi \right) + \dots,$$

where ellipses indicate Umklapp and band-curvature terms present in the XXZ model.

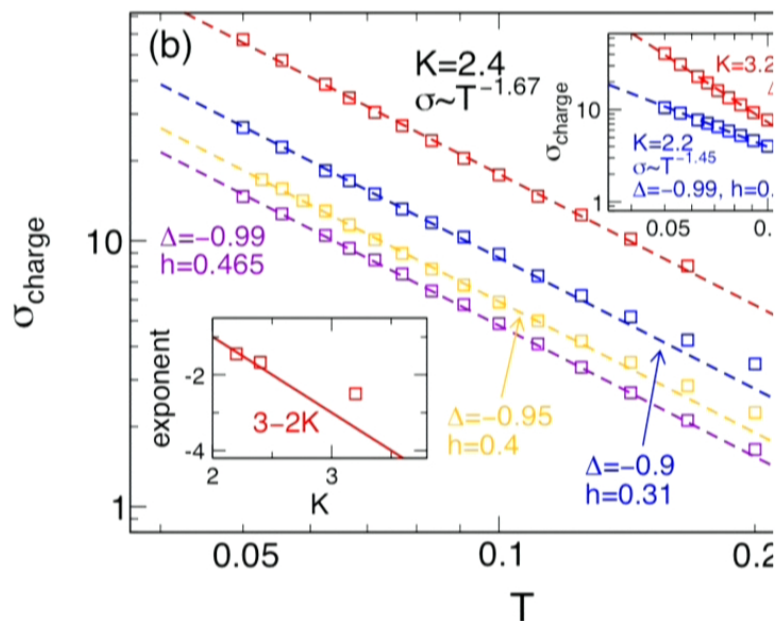
We know that simple bosonization analysis of the Umklapp term is actually incorrect, because integrability leads to a non-zero Drude weight. Does adding the new cosine make the scaling prediction valid?

$$\sigma_c = h^{-2} T^{3-2K} / C(K)$$

$$C(K) = \pi^{K-1} (1 - K^{-1}/2)^{2K-1} \cos^2(\pi K/2) \\ \times \sin^{1-2K}(\pi K^{-1}/2) \Gamma^2(K/2) \Gamma^2(1/2 - K/2) \\ \times \Gamma^{2K} \left(\frac{1}{4K-2} \right) \Gamma^{-2K} \left(\frac{1}{2-K^{-1}} \right) \exp \left(2 \int_0^{+\infty} \frac{dx}{x} \right. \\ \left. \times \left(1 - (K-1)e^{-2x} - \frac{\sinh x}{\sinh((K^{-1}-1)x) + \sinh x} \right) \right).$$

Conductivity scaling

$$\sigma = \lim_{t_M \rightarrow \infty} \lim_{L \rightarrow \infty} \frac{1}{LT} \operatorname{Re} \int_0^{t_M} \langle J(t)J(0) \rangle dt.$$



For K not too large, linear prediction is self-consistent and power-laws are observed that are consistent with bosonization predictions.

Puzzle: possible *thermal* Drude weight in a nonintegrable dimerized chain; no obvious reason it should exist.

Bosonization models

Bosonization analysis: \hbar just generates a new cosine:

$$H = \frac{v}{2} \int dx \left(\Pi^2 + (\partial_x \phi)^2 \right) + c\hbar \int dx \cos \left(2\sqrt{\pi K} \phi \right) + \dots,$$

where ellipses indicate Umklapp and band-curvature terms present in the XXZ model.

Our model is a modified version of Sirkar, Pereira, Affleck: it assumes the operators created by \hbar are alone sufficient to break integrability (the “single-operator” theory). This is consistent with the data.

However, another viable possibility is the “two-operator” theory of Rosch and Andrei: it is only the combination of \hbar and umklapp that breaks integrability, which leads to non-commuting $\hbar \rightarrow 0$ and $T \rightarrow 0$ limits.

It could be that we are always in the small- \hbar limit, and that if we went to much lower temperatures at fixed \hbar , we would see a different exponent--subject for future investigation.

Bosonization models

Bosonization analysis: \hbar just generates a new cosine:

$$H = \frac{v}{2} \int dx \left(\Pi^2 + (\partial_x \phi)^2 \right) + c\hbar \int dx \cos \left(2\sqrt{\pi K} \phi \right) + \dots,$$

where ellipses indicate Umklapp and band-curvature terms present in the XXZ model.

Our model is a modified version of Sirkar, Pereira, Affleck: it assumes the operators created by \hbar are alone sufficient to break integrability (the “single-operator” theory). This is consistent with the data.

However, another viable possibility is the “two-operator” theory of Rosch and Andrei: it is only the combination of \hbar and umklapp that breaks integrability, which leads to non-commuting $\hbar \rightarrow 0$ and $T \rightarrow 0$ limits.

It could be that we are always in the small- \hbar limit, and that if we went to much lower temperatures at fixed \hbar , we would see a different exponent--subject for future investigation.

What about non-equilibrium transport?

1. Create two different temperatures in two disconnected, infinite 1D “leads”.
2. Connect them by a finite region (e.g., one bond).
3. Evolve in time for as long as possible.

Is a steady-state heat current reached?

Is non-equilibrium (finite bias) thermal transport determined by linear-response thermal conductance?

We observe two different outcomes, depending on integrability of the leads and whether the connected system is homogeneous.

What about non-equilibrium transport?

1. Create two different temperatures in two disconnected, infinite 1D “leads”.
2. Connect them by a finite region (e.g., one bond).
3. Evolve in time for as long as possible.

Is a steady-state heat current reached?

Is non-equilibrium (finite bias) thermal transport determined by linear-response thermal conductance?

We observe two different outcomes, depending on integrability of the leads and whether the connected system is homogeneous.

$t < 0$

T_1

T_2

$t > 0$

∞



Linear and non-linear response

When the finite system is homogeneous and the leads have a nonzero Drude weight, we find:

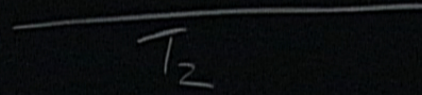
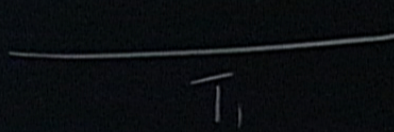
1. there is a steady state;
2. there is a function f such that

$$\lim_{t \rightarrow \infty} \langle J_E(n, t) \rangle = f(T_L) - f(T_R)$$

In other words, linear response $G = \partial_T f$ is sufficient to determine non-linear response.

For a CFT (Bernard & Doyon, Cardy), this was known, and f goes as T^2 for small T , $1/T$ for large T . (“1D black-body”)

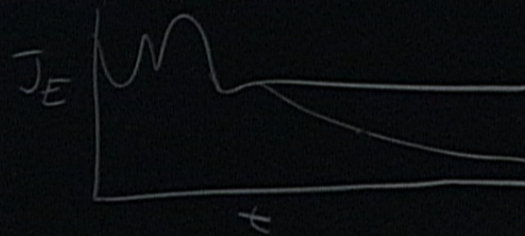
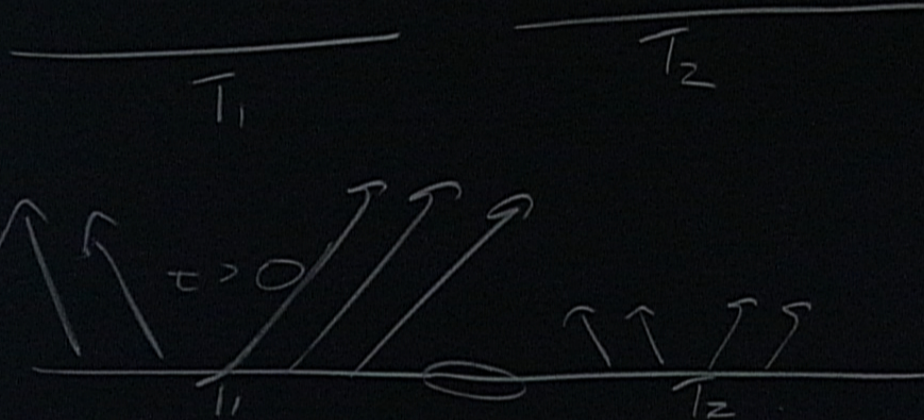
$$t < 0$$



$$t > 0$$



$t < 0$



$$J_E(x) = -k(T(x)) \nabla T$$

Linear and non-linear response

When the finite system is homogeneous and the leads have a nonzero Drude weight, we find:

1. there is a steady state;
2. there is a function f such that

$$\lim_{t \rightarrow \infty} \langle J_E(n, t) \rangle = f(T_L) - f(T_R)$$

In other words, linear response $G = \partial_T f$ is sufficient to determine non-linear response.

For a CFT (Bernard & Doyon, Cardy), this was known, and f goes as T^2 for small T , $1/T$ for large T . (“1D black-body”)

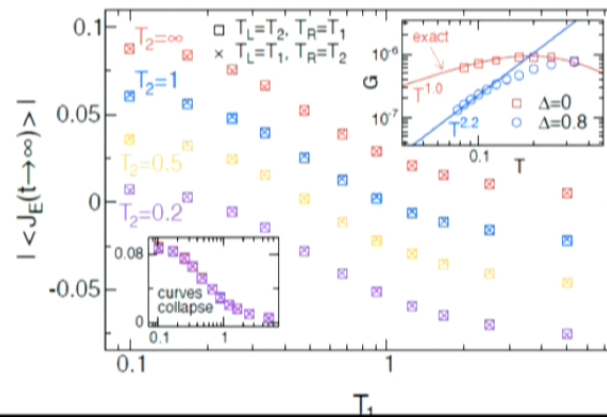
Linear and non-linear response

2. there is a function f such that

$$\lim_{t \rightarrow \infty} \langle J_E(n, t) \rangle = f(T_L) - f(T_R)$$

Makes testable predictions, e.g.,

$$J_E(T_1 \rightarrow T_3) = J_E(T_1 \rightarrow T_2) + J_E(T_2 \rightarrow T_3)$$



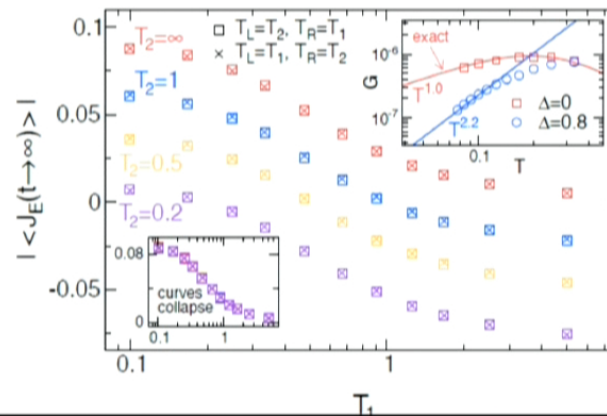
Linear and non-linear response

2. there is a function f such that

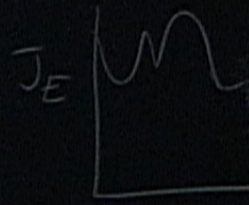
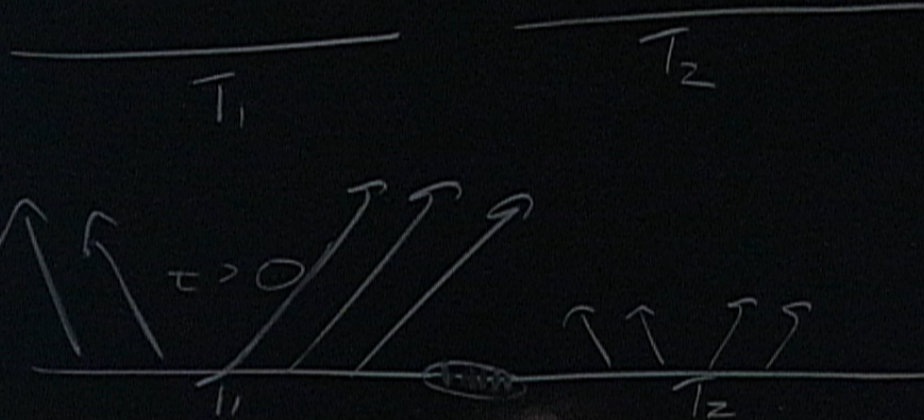
$$\lim_{t \rightarrow \infty} \langle J_E(n, t) \rangle = f(T_L) - f(T_R)$$

Makes testable predictions, e.g.,

$$J_E(T_1 \rightarrow T_3) = J_E(T_1 \rightarrow T_2) + J_E(T_2 \rightarrow T_3)$$

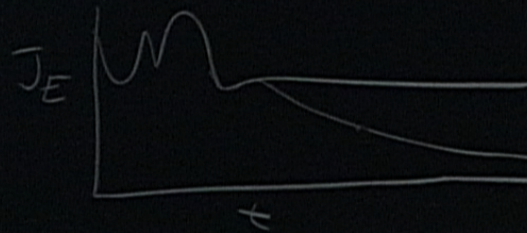
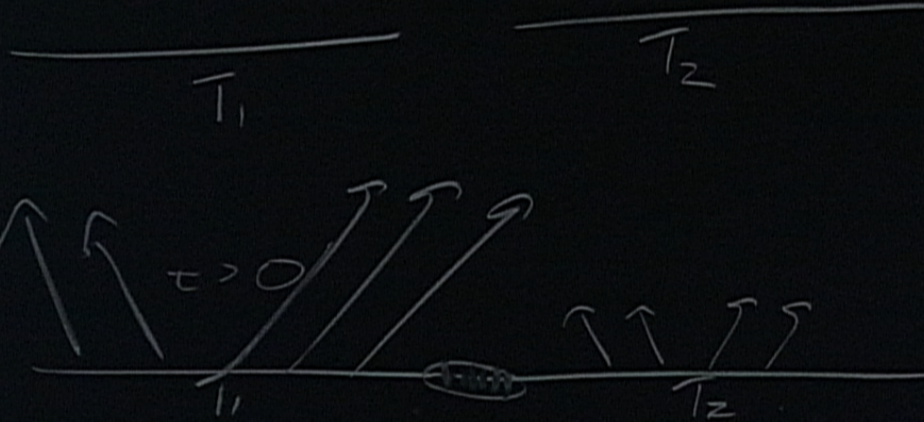


$t < 0$



$$J_E(x) = -k(T(x)) \nabla T$$

$t < 0$



$$J_E(x) = -k(T(x)) \frac{\partial T}{\partial x}$$

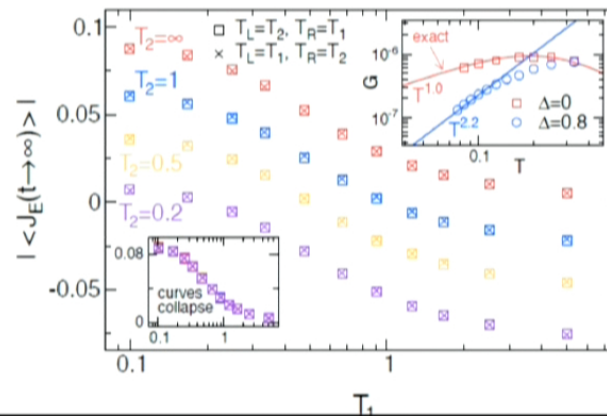
Linear and non-linear response

2. there is a function f such that

$$\lim_{t \rightarrow \infty} \langle J_E(n, t) \rangle = f(T_L) - f(T_R)$$

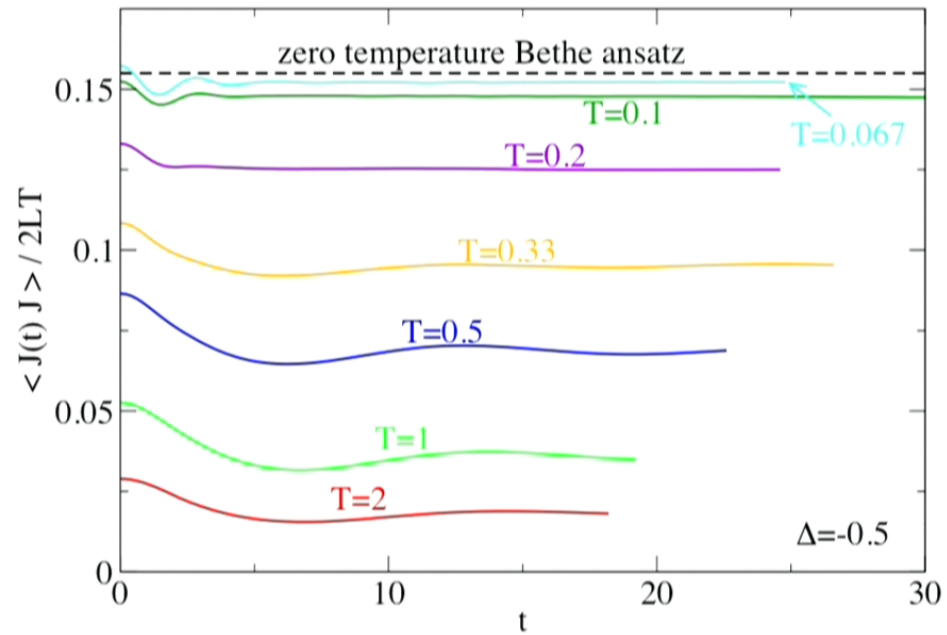
Makes testable predictions, e.g.,

$$J_E(T_1 \rightarrow T_3) = J_E(T_1 \rightarrow T_2) + J_E(T_2 \rightarrow T_3)$$



Drude weight of XXZ model

$$\sigma(\omega) = D\delta(\omega) + \dots$$



Time-dependent matrix-product-state numerics using an “entanglement-based” trick

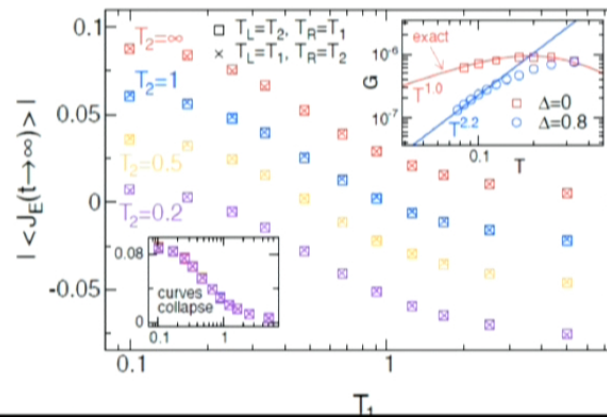
Linear and non-linear response

2. there is a function f such that

$$\lim_{t \rightarrow \infty} \langle J_E(n, t) \rangle = f(T_L) - f(T_R)$$

Makes testable predictions, e.g.,

$$J_E(T_1 \rightarrow T_3) = J_E(T_1 \rightarrow T_2) + J_E(T_2 \rightarrow T_3)$$



Intro to disordered electronic systems

For non-interacting systems, we understand essentially completely the effects of disorder.

For the simplest symmetries (orthogonal and unitary ensembles), disorder is localizing for essentially all states in 1D and 2D.

Real experimental systems typically have “dephasing” from interactions with phonons, which ultimately leads to a finite diffusion constant.

The combination of interactions and disorder in closed systems (“many-body localization”) is not well understood even in 1D.

are the only two possibilities diffusive and localized? can there be subdiffusive scaling? (“glassy”: $r \sim \log t$)

Fully coherent dynamics is potentially relevant in atomic experiments.

(Gapped topological phases have “protected” surface states, i.e., no localization.)

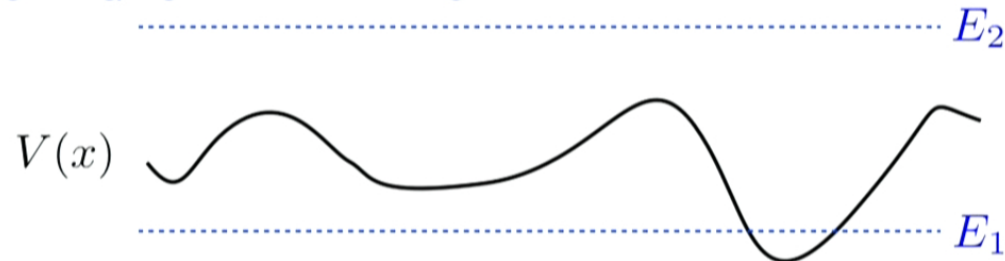
Intro to disordered electronic systems

Consider a quantum particle, described by the Schrödinger equation, moving in a random potential.

Intuitively, we might expect:

at low energy, eigenstates are trapped (“localized”) in potential minima

at high energy, eigenstates are scattering states

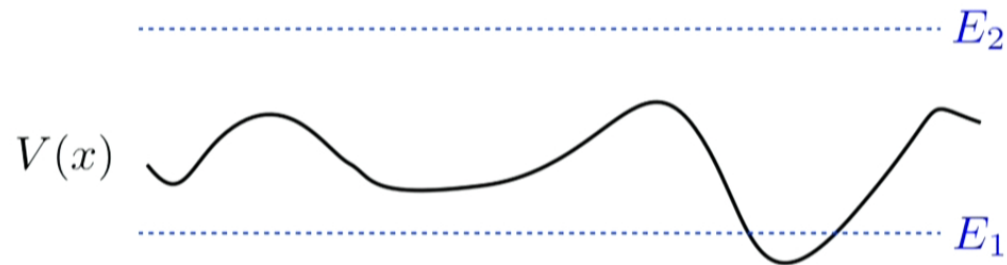


In 3D, this intuition is basically correct, and there is a specific energy (the “mobility edge”) that separates localized from disordered states.

Argument for mobility edge: (Mott) coexistence of localized and extended states at same energy is unstable, as a small perturbation will mix and give only extended states.

Intro to disordered electronic systems

This intuition breaks down in one or two dimensions: all electronic states are localized up to arbitrarily high energies, although the localization length increases with E .



Why is 2D special? Consider the stability of scattering states. We can model the scattering state as a random walk.

A random walk above 2D revisits any point only a finite number of times on average, so a weak potential fluctuation cannot be amplified infinitely. In 2D or below, a point (say the starting point) is visited an infinite number of times, and a “weak” potential can become strong.

Intro to disordered electronic systems

So one-particle localization is very sensitive to dimensionality.

It is also sensitive to *symmetries*. For example, if we broke time-reversal symmetry with a magnetic field, then in 2D extended states survive at isolated energies.

If we assume that disorder breaks all symmetries except for two discrete symmetries T (time reversal) and C (chiral/charge conjugation), and that each of these can square to $+1$ or -1 if present, then there are 10 symmetry classes.

Why 10?

Just considering T gives 3 “Wigner-Dyson” classes: orthogonal ($T^2 = +1$), symplectic ($T^2 = -1$), and unitary (T broken).

Adding C gives 9 classes (3 times 3). There is also the possibility of having CT symmetry without either C or T separately, hence 10 “Altland-Zirnbauer” classes.

How do we see localization experimentally?

Why is it important for some basic physics questions?

Is there more to the story than symmetry and dimensionality?

Spontaneous symmetry breaking in a quenched ferromagnetic spinor Bose-Einstein condensate

L. E. Sadler¹, J. M. Higbie¹, S. R. Leslie¹, M. Vengalattore¹ & D. M. Stamper-Kurn¹

A central goal in condensed matter and modern atomic physics is the exploration of quantum phases of matter—in particular, how the universal characteristics of zero-temperature quantum phase transitions differ from those established for thermal phase transitions at non-zero temperature. Compared to conventional condensed matter systems, atomic gases provide a unique opportunity to explore quantum dynamics far from equilibrium. For example, gaseous spinor Bose-Einstein condensates^{1–3} (whose atoms have non-zero internal angular momentum) are quantum fluids that simultaneously realize superfluidity and magnetism, both of which are associated with symmetry breaking. Here we explore spontaneous symmetry breaking in ⁸⁷Rb spinor condensates, rapidly quenched across a quantum phase transition to a ferromagnetic state. We observe the formation of spin textures, ferromagnetic domains and domain walls, and demonstrate phase-sensitive *in situ* detection of spin vortices. The latter are topological defects resulting from the symmetry breaking, containing non-zero spin current but no net mass current⁴.

Spinor atomic gases^{1–3} are those comprised of atoms with non-

quench, high-resolution maps of the magnetization vector density were obtained using magnetization-sensitive phase-contrast imaging⁵. After the quench, transverse ferromagnetic domains of variable size formed spontaneously throughout the condensate, divided by narrow unmagnetized domain walls. Concurrent with the formation of these domains, we also observed topological defects that we characterize as singly charged spin vortices with circulating spin currents and unmagnetized filled cores.

Spinor BECs in the $|F = 1, m_z = 0\rangle$ hyperfine state were confined in an optical dipole trap characterized by oscillation frequencies $(\omega_x, \omega_y, \omega_z) = 2\pi(56, 350, 4.3) \text{ s}^{-1}$. The condensates, typically containing $2.1(1) \times 10^6$ atoms, were formed at a magnetic field of 2 G and characterized by a peak density $n_0 = 2.8 \times 10^{14} \text{ cm}^{-3}$ and Thomas-Fermi radii $(r_x, r_y, r_z) = (12.8, 2.0, 167) \mu\text{m}$ (see Methods). Variations in the internal-state wavefunction were constrained in these anisotropic condensates to just two spatial dimensions (\hat{x} and \hat{z}) because the spin healing length, $\xi_s = \sqrt{\hbar^2/2m|c_2|n_0} = 2.4 \mu\text{m}$, was larger than the cloud size r_y in the \hat{y} direction. Thus, imaging the condensate in the \hat{x} - \hat{z} plane produced complete maps of the magnetization

Phase-ordering kinetics after quenching across a quantum phase transition

See also experiments by Weiss et al. on thermalization; DeMarco and Inguscio on disordered atomic gases and localization. (Modugno, Inguscio et al. is closest to what we will talk about later.)

Here we want to focus on the basic question

Does an isolated quantum system with interactions and disorder show localization?

which is related to the equally basic question

When do isolated quantum systems thermalize?

The connection is that localization is the most plausible physical way to avoid thermalization: localized particles cannot move around and equilibrate. In a delocalized system, we expect that a test particle sees other particles as a thermal “bath”.

Besides symmetry and dimensionality, what else controls localization?

Many-body localization at infinite temperature

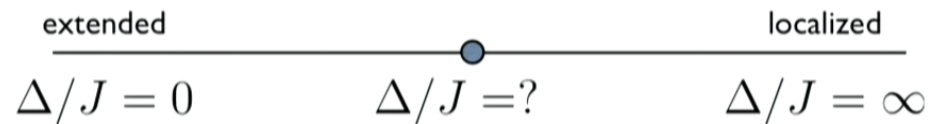
$$H = J_{xx} \sum_i (S_i^x S_{i+1}^x + S_i^y S_{i+1}^y) + J_z \sum_i S_i^z S_{i+1}^z + \sum_i h_i S_i^z$$

Clean XXZ chain + random z-directed Zeeman field

$$h_i \in (-\Delta, \Delta)$$

Claim: look at “infinite-temperature” dynamics but with no dephasing;
evolve an arbitrary initial state by the Schrödinger equation

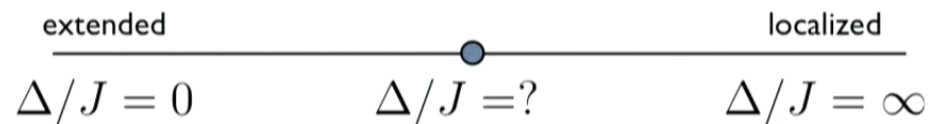
Heisenberg phase diagram:



Many-body localization at infinite temperature

$$H = J_{xx} \sum_i (S_i^x S_{i+1}^x + S_i^y S_{i+1}^y) + J_z \sum_i S_i^z S_{i+1}^z + \sum_i h_i S_i^z$$

Heisenberg phase diagram:



Transition should be detectable in:

level statistics: (Wigner-Dyson vs. Poisson) [Oganesyan & Huse, 2008](#)

dynamical correlation functions

correlation distributions [Pal & Huse, 2010](#); [Reichman et al. 2010](#)

entanglement growth/thermalization

This spin chain problem is a numerically easier reformulation of many-body localization in continuum Fermi systems at nonzero T ([Basko, Aleiner, Altshuler 2007](#))

Should be generic for 1D local interactions, disorder, U(1) symmetry.

Many-body localization at infinite temperature

$$H = J_{xx} \sum_i (S_i^x S_{i+1}^x + S_i^y S_{i+1}^y) + J_z \sum_i S_i^z S_{i+1}^z + \sum_i h_i S_i^z$$

Numerical experiment: start with an arbitrary product state (local S_z eigenstate) and evolve under H . Can view as a “global quench”.

“*Extended phase*”: expect S grows linearly with t (Calabrese and Cardy)

“*One-particle localized phase*”: ($J_z = 0$) eigenstates are Slater determinants of localized one-particle states; S saturates to a finite value.

What happens if we add interactions to the localized phase?

Note: this is efficiently simulable because for early times the system has small entanglement (Prelovsek et al., 2007)

Many-body localization at infinite temperature

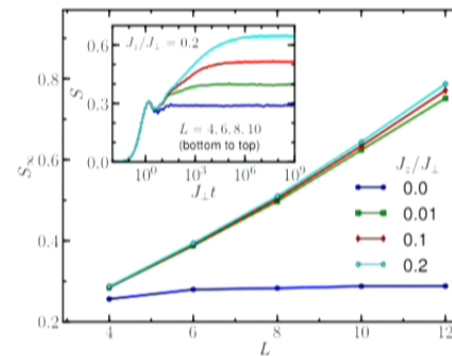
$$H = J_{xx} \sum_i (S_i^x S_{i+1}^x + S_i^y S_{i+1}^y) + J_z \sum_i S_i^z S_{i+1}^z + \sum_i h_i S_i^z$$

What does entanglement entropy growth mean?

The entanglement entropy comes from the reduced density matrix, which governs any local experiment.

So any measurement of entropy in a subsystem will show that the interacting system is “more thermalized” than the Anderson one.

However, studies of the saturation of small blocks suggest that the full thermal entropy is not reached: $O(L)$ but small.



Many-body localization at infinite temperature

$$H = J_{xx} \sum_i (S_i^x S_{i+1}^x + S_i^y S_{i+1}^y) + J_z \sum_i S_i^z S_{i+1}^z + \sum_i h_i S_i^z$$

Numerical experiment: start with an arbitrary z-product state (local S_z eigenstate) and evolve under H . Can view as a “global quench”.

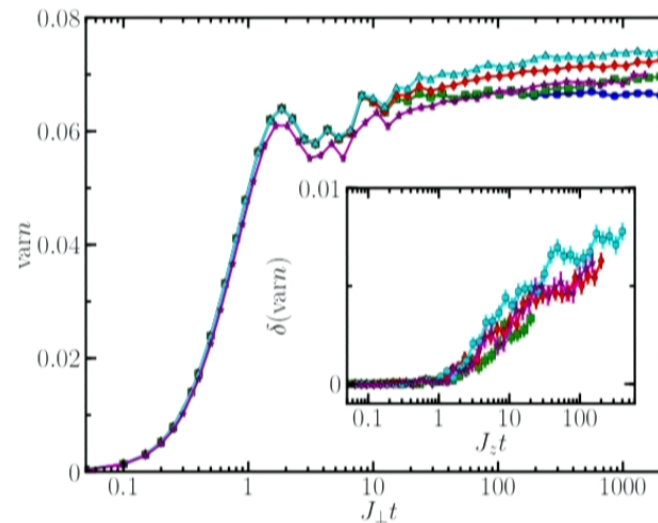
What about transport of the U(1) quantity?

Effect of interactions is less obviously singular--it could be that conductivity is zero.

We cannot rule out that the only physics with interactions is extended and that there is eventually thermalization.

But there is a long, possibly infinite, time range over which dynamics is very slow.

(Slower log log dynamics at low energy in random singlet phase--Iglói et al. PRB 2012)



Many-body localization at infinite temperature

Possible interpretations:

1. There is a many-body-localized phase (MBL) that is like the Anderson localized phase.

No, since the MBL phase has dynamics with a diverging length scale.

The Anderson localized phase saturates to exponential accuracy in finite time (the time required for a particle to travel the localization length).

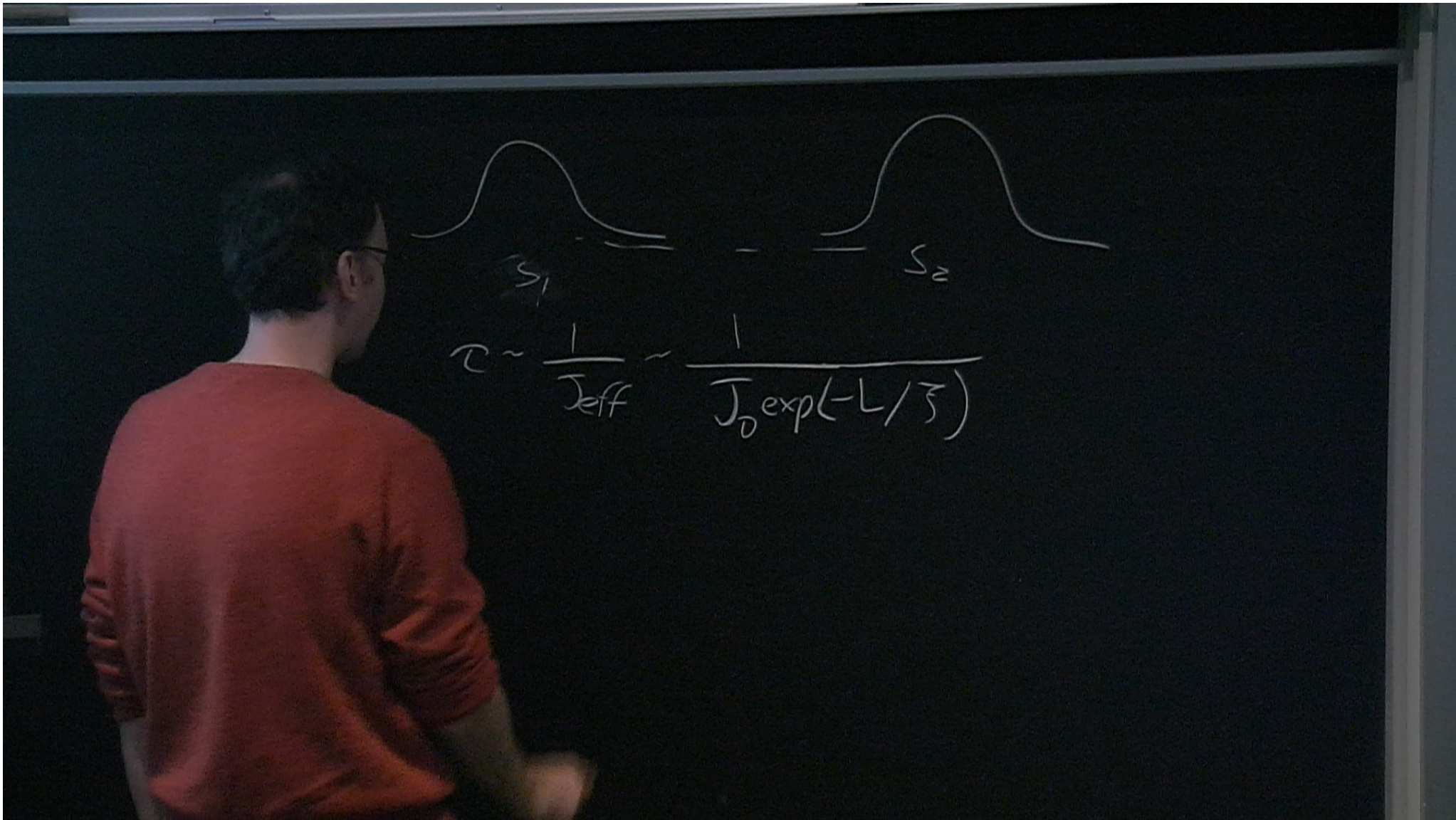
2. The MBL phase has localized particles but glassy dynamics. It evolves toward “local equilibrium”, like a GGE with local temperature.

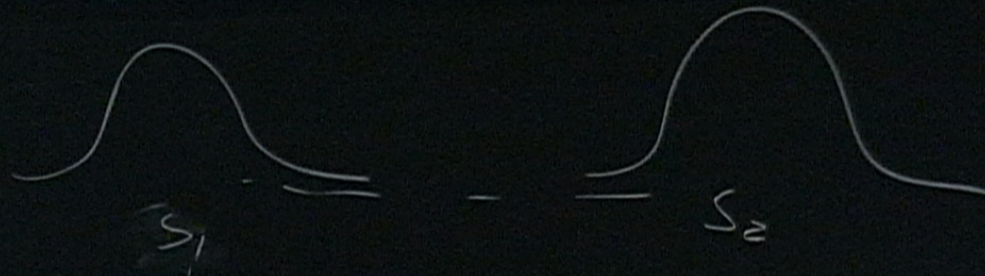
3. The MBL phase has particles that continue to move but in a sub-diffusive way (e.g., $r \sim \log^2 t$, as in Sinai diffusion). This would still have zero conductivity but might thermalize.

4. There is no sharply defined MBL phase.

Open question: does the state eventually thermalize? Entanglement entropy and spectrum should approach ETH* predictions.

ETH=“eigenstate thermalization hypothesis”





$$\tau \sim \frac{1}{J_{\text{eff}}} \sim \frac{1}{J_0 \exp(-L/\xi)}$$

$$S \sim L \sim \xi \log(J_0 t)$$

Many-body localization at infinite temperature

$$H = J_{xx} \sum_i (S_i^x S_{i+1}^x + S_i^y S_{i+1}^y) + J_z \sum_i S_i^z S_{i+1}^z + \sum_i h_i S_i^z$$

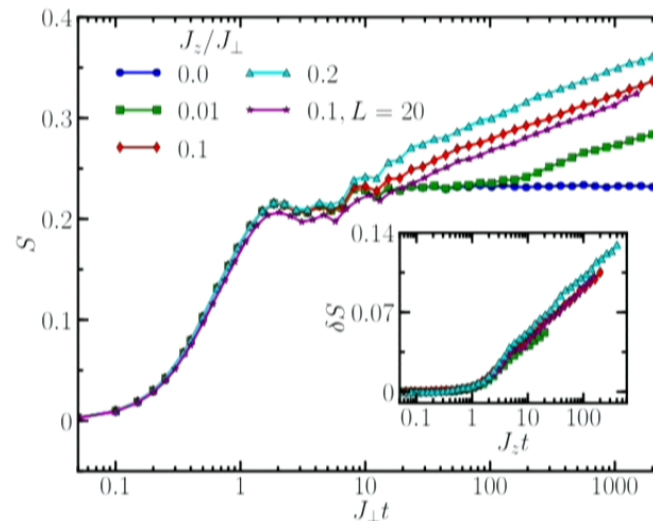
Numerical experiment: start with an arbitrary z-product state (local S_z eigenstate) and evolve under H . Can view as a “global quench”.

Half-chain entanglement saturates with no interactions.

Interactions increase entanglement growth (consistent with previous work: De Chiara et al., Prelovsek et al.).

Surprise:
Interactions are a singular perturbation.

Even a very weak interaction leads eventually to a *slow but unbounded* increase of entanglement.



Many-body localization at infinite temperature

$$H = J_{xx} \sum_i (S_i^x S_{i+1}^x + S_i^y S_{i+1}^y) + J_z \sum_i S_i^z S_{i+1}^z + \sum_i h_i S_i^z$$

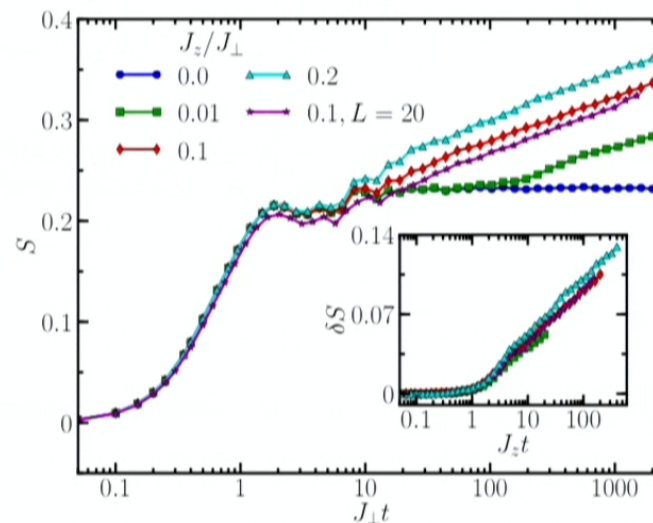
Numerical experiment: start with an arbitrary z-product state (local S_z eigenstate) and evolve under H . Can view as a “global quench”.

Half-chain entanglement saturates with no interactions.

Interactions increase entanglement growth (consistent with previous work: De Chiara et al., Prelovsek et al.).

Surprise:
Interactions are a singular perturbation.

Even a very weak interaction leads eventually to a *slow but unbounded* increase of entanglement.



Plateau behavior in FQHE r edge tunneling

A. M.Chang et al., PRL 2001

Fitting required even to see plateaus clearly, and the exponents in some samples are displaced relative to theory; other samples seem roughly to agree with theory.

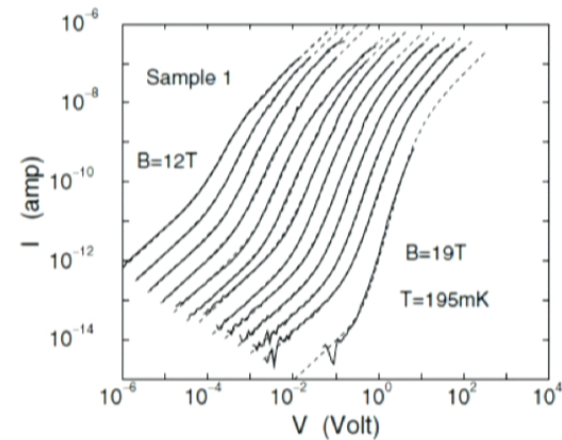


FIG. 2. Log-log plot of the I - V characteristics (solid lines) for electron tunneling from the FQH edge into the bulk doped $n + \text{GaAs}$ in sample 1 at various magnetic fields from 12 to 19 T in steps of 0.5, 18, and 18.5 T excluded. Corresponding filling factors vary from 2.69 to 4.26. Dashed lines represent best fits to Eq. (1). Successive curves are shifted by 0.3 units (a factor of 2) in the x direction for clarity.

Topological field theory of QHE

How can we describe the topological order in the quantum Hall effect?

Standard answer: Chern-Simons theory
(Girvin & MacDonald; Zhang, Hansson, and Kivelson; Read; ...)

$$L_{CS} = -\frac{k}{4\pi} \varepsilon^{\mu\nu\lambda} a_\mu \partial_\nu a_\lambda + j^\mu a_\mu, \quad j^\mu = \frac{1}{2\pi} \varepsilon^{\mu\nu\lambda} \partial_\nu A_\lambda$$

There is an "internal gauge field" a that couples to electromagnetic A .

Integrating out the internal gauge field a gives a Chern-Simons term for A , which just describes a quantum Hall effect:

$$L_{QHE} = -\frac{1}{4k\pi} \varepsilon^{\mu\nu\lambda} A_\mu \partial_\nu A_\lambda$$

There is a difference in principle between the topological field theory and the topological term generated for electromagnetism; they are both Chern-Simons terms.

Topological field theory of QHE

How can we describe the topological order in the quantum Hall effect?

Standard answer: Chern-Simons theory
(Girvin & MacDonald; Zhang, Hansson, and Kivelson; Read; ...)

$$L_{CS} = -\frac{k}{4\pi} \varepsilon^{\mu\nu\lambda} a_\mu \partial_\nu a_\lambda + j^\mu a_\mu, \quad j^\mu = \frac{1}{2\pi} \varepsilon^{\mu\nu\lambda} \partial_\nu A_\lambda$$

There is an "internal gauge field" a that couples to electromagnetic A .

Integrating out the internal gauge field a gives a Chern-Simons term for A , which just describes a quantum Hall effect:

$$L_{QHE} = -\frac{1}{4k\pi} \varepsilon^{\mu\nu\lambda} A_\mu \partial_\nu A_\lambda$$

There is a difference in principle between the topological field theory and the topological term generated for electromagnetism; they are both Chern-Simons terms.

Topological field theory of QHE

What good is the Chern-Simons theory? (Wen)

$$L_{CS} = -\frac{k}{4\pi} \varepsilon^{\mu\nu\lambda} a_\mu \partial_\nu a_\lambda + j^\mu a_\mu, \quad j^\mu = \frac{1}{2\pi} \varepsilon^{\mu\nu\lambda} \partial_\nu A_\lambda$$

The bulk Chern-Simons term is not gauge-invariant on a manifold with boundary.

It predicts that a quantum Hall droplet must have a chiral boson theory at the edge:

$$S = \frac{k}{4\pi} \int \partial_x \phi (\partial_t \phi - v \partial_x \phi) dx dt$$

For fractional quantum Hall states, the chiral boson is a "Luttinger liquid" with strongly non-Ohmic tunneling behavior, e.g., $I \sim V^3$ for Laughlin state at $1/3$.

Experimentally this is seen qualitatively--perhaps not quantitatively.

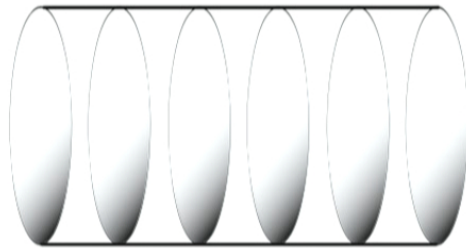
DMRG for FQHE edges

Put LL on a cylinder: get an unusual spinless fermion model with interaction range determined by the cylinder size.

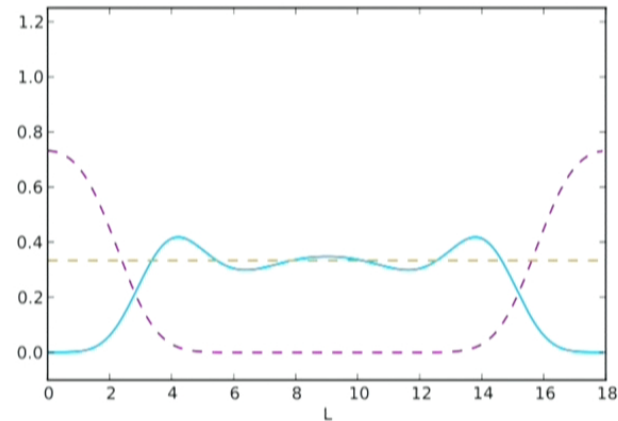
[Zaletel, Mong, Pollmann arXiv](#)

Add a confining potential around the cylinder to create edges.

[Zaletel, Varjas, JEM, unpublished](#)



electron density
nonuniform



1/3 state:
density profile

DMRG for FQHE edges

Wen's theory predicts that the edge electrons should have strongly non-Fermi liquid correlations.

With ED, one gets a discrete spectrum; hard to confirm expt.

Now the edges run along the infinite cylinder: continuous spectrum

1/3 edge:

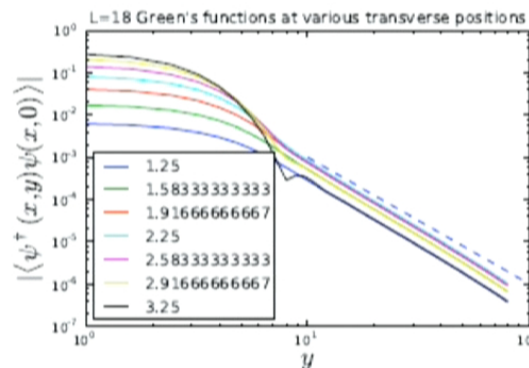
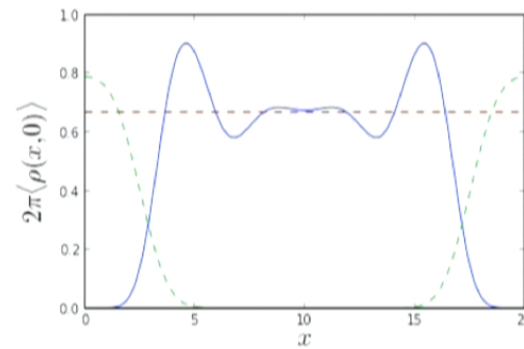


FIGURE 3. $G(y;x)$ at $L = 18$, $\eta = 3$ given by dashed line.

DMRG for FQHE edges

Can observe more complicated multicondensate behavior and nonuniversality of edge exponent: $2/3$ spin-polarized state

$2/3$ density:
 $1/3$ gas of holes
in filled Landau level



DMRG for FQHE edges

One surprise: multicomponent “fractional Luttinger theorem” (apparently conjectured by Haldane in 1990s).

The $n(ky)$ distribution looks like the $n(x)$ distribution deconvolved with a Gaussian. This reveals discontinuities of the derivative.

For a conventional 1D metal, “Luttinger’s theorem” says that the location of the singular momentum is fixed by the density and unrenormalized by interactions.

In our 1D effective Hamiltonians, something similar happens: for example, in the $2/5$ state,

$$\nu_{1D} = \frac{2k_1}{3} + \frac{2k_2}{15}$$

This holds even when edge exponents are modified, so perhaps can be used to define FQHE physics in a wire.

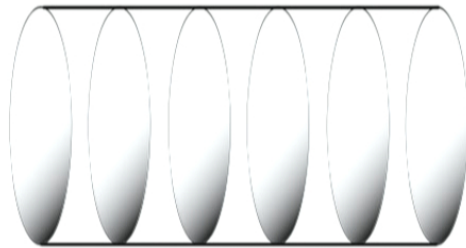
DMRG for FQHE edges

Put LL on a cylinder: get an unusual spinless fermion model with interaction range determined by the cylinder size.

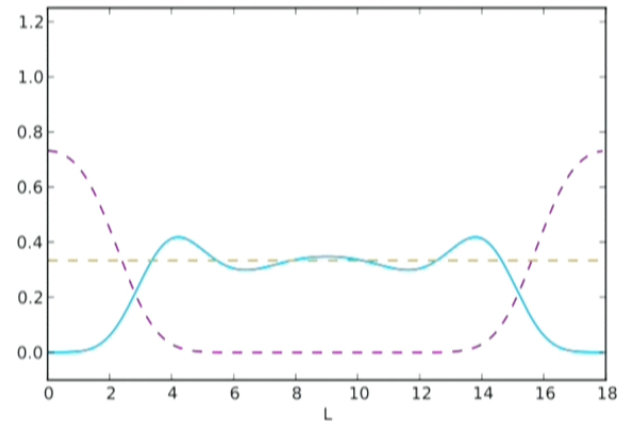
[Zaletel, Mong, Pollmann arXiv](#)

Add a confining potential around the cylinder to create edges.

[Zaletel, Varjas, JEM, unpublished](#)



electron density
nonuniform



1/3 state:
density profile

DMRG for FQHE edges

One surprise: multicomponent “fractional Luttinger theorem” (apparently conjectured by Haldane in 1990s).

The $n(ky)$ distribution looks like the $n(x)$ distribution deconvolved with a Gaussian. This reveals discontinuities of the derivative.

For a conventional 1D metal, “Luttinger’s theorem” says that the location of the singular momentum is fixed by the density and unrenormalized by interactions.

In our 1D effective Hamiltonians, something similar happens: for example, in the $2/5$ state,

$$\nu_{1D} = \frac{2k_1}{3} + \frac{2k_2}{15}$$

This holds even when edge exponents are modified, so perhaps can be used to define FQHE physics in a wire.